

Microstructural, mechanical and corrosion properties of two cast binary cobalt-chromium alloys base of real dental alloys for prosthetic dentistry

Princilia Billy¹, Patrice Berthod^{1,2*}

¹Faculty of Sciences and Technologies, University of Lorraine, B.P. 70239, 54506 Vandoeuvre-lès-Nancy (FRANCE)

²Institut Jean Lamour (UMR CNRS 7198), University of Lorraine, B.P. 70239, 54506 Vandoeuvre-lès-Nancy – (FRANCE)

E-mail: Patrice.Berthod@univ-lorraine.fr

ABSTRACT

Cobalt-based alloys containing chromium in quantity high enough represent a family of rather cheap dental alloys, besides the maybe well-known nickel-based family. They are able to bring mechanical properties and corrosion resistance high enough to be used in prosthetic dentistry instead much more expensive alloys based on noble metals. After a recent study concerning two simple nickel-chromium alloys derived from commercial dental alloys, this aim of this work is to reproduce the same tests on binary cobalt-chromium alloys, a first one itself simplified version of another commercial alloy, and a second one containing less chromium. Elaboration by casting, hardness and compression characterization, and evaluation of the corrosion behaviour in a simple artificial saliva by the means of electrochemical techniques, allowed seeing that the Co-15wt.%Cr alloy was better than the Co-30Cwt.%Cr one simultaneously in term of mechanical properties and of corrosion behaviour. It may represent an interesting base for new more complex cobalt-based alloys.

© 2016 Trade Science Inc. - INDIA

KEYWORDS

Cobalt-chromium alloys;
Mechanical properties;
Electrochemical measurements;
Artificial saliva.

INTRODUCTION

Besides the dental alloys based on very noble metals such as gold, platinum and palladium, several manufacturer's also propose alloys which are not so expensive although they bring their good mechanical properties and excellent corrosion resistance to prosthetic applications such as the frameworks which strengthened fixed partial denture or

removable prostheses. Among them, there are {nickel-chromium}-based alloys but also less common alloys based on cobalt. Cobalt-alloys, elsewhere used in other medical fields such as bone surgery^[1], are also considered for dental applications^[2-4] since several decades. Their characteristics such as microstructures^[5,6], mechanical properties^[7,8] and resistance against corrosion in the buccal milieu^[7, 9] are subjected to investigations since many years. The

Full Paper

purpose of the present work is, in the continuity of recent studies^[10,11] devoted to the dSIGN30 (90Co-30Cr-4Ga-3Nb), to carry out on a simplified version of the latter alloy the same characterizations as shortly done on the nickel-based 4ALL alloy^[12], concerning microstructure, compression properties, and corrosion in a solution simulating saliva, with special attention to the effect of the Cr content and, especially for corrosion, of a plastic deformation.

EXPERIMENTAL

Elaboration of the alloys

Two alloys were preliminarily elaborated by foundry. Parts of pure elements (Co and Cr, mainly from Alfa Aesar, >99.9 wt.%) were separately weighed to obtain about two 40 grams charges, in order to constitute two binary alloys: a Co-15wt.%Cr and a Co-30wt.%Cr one. Each charge was placed in the water-cooled crucible of a High Frequency Induction furnace (CELES), which was thereafter isolated from laboratory air by a silica tube in which three cycles $\{7 \times 10^{-2}$ mbar – vacuum; incorporation of 600 mbars of pure Argon} were applied. To finish the internal atmosphere was stabilized to 300 mbars of pure Ar. Melting of the charge and homogenization were achieved by heating upto about 4kV and almost isothermal stage during three minutes in the liquid state. Rather fast cooling led to solidification and solid state cooling, of a compact ingot.

Machining, metallography preparation and observations

The two ingots were cut in order to obtain different types of samples. Two about $\{5.5 \text{ mm} \times 5.5 \text{ mm} \times 4 \text{ mm}\}$ -parallelepipeds were machined in each ingot. In both cases one of the two parts was devoted to metallographic characterization and the second one was kept for specifying the mechanical behaviour compression.

The parts destined for metallography were first embedded in a cold resin mixture (82% of CY230 resin and 18% of HY253 hardener, liquid products from ESCIL®). After total stiffening and extraction outside the plastic mould the obtained mounted

samples were ground with SiC papers from 120-grit upto 2400-4000-grit. After ultrasonic cleaning they were polished with textile disk enriched with $1 \mu\text{m}$ hard particles until obtaining a mirror-like state.

The observations were done by electron microscopy. A Scanning Electron Microscope (SEM) from JEOL (JSM 6010LA model), equipped with an Energy Dispersion Spectrometer (EDS), allowed observations in Back Scattered Electrons (BSE) mode and semi-quantitative chemical analysis (full frame and spot), under a 20kV acceleration voltage.

Mechanical properties

The hardness of the two alloys was first specified. This was done by performing Vickers indentation under a 10kg-load, three times per alloy. This allowed obtaining an average value and a standard deviation one.

The parallelepipeds especially machined for that were subjected to compression test allowing a plastic deformation important enough to get a hardened version of the same alloys. Several properties were deduced from the obtained compression curves: the yield strength (transition from the elastic deformation to the plastic one) and the hardening parameters (k and n) involved in the Ludwig's equation (eq. 1):

$$\sigma = k \times \epsilon^n \quad (1)$$

They can be easily deduced of the straight line resulting from the $\ln(\sigma)$ versus $\ln(\epsilon)$ plotting since the logarithm of k is its ordinate at the origin while n is its slope (eq. 2).

$$\ln(\sigma) = \ln(k) + n \times \ln(\epsilon) \quad (2)$$

Corrosion properties

For each alloy an as-cast parallelepiped part and the plastically deformed parallelepiped parts were immersed in a liquid cold resin mixture but without submersion as for the metallographic samples. After total stiffening they were extracted from the plastic mould. They were placed in a vice, sewed a little and the denuded part of an electrical wire was inserted in the resulting slot by compression. Incorporated again in the mould additional liquid cold resin mixture was poured to totally immerse the upper part of the sample as well as the denuded copper. The metallic part of the obtained electrode was then

ground until the 1200-grit paper, washed and dried.

Two types of electrochemical tests were carried out, using the model 263A potentiostat of Princeton Applied Research driven by the M352 software of EGG/Princeton:

Measurement of the Open Circuit potential (E_{ocp}) followed by a linear polarization from $E_{ocp} - 20\text{mV}$ up to $E_{ocp} + 20\text{mV}$ at the constant rate of $+10\text{mV/min}$, to determine the polarization resistance R_p (from the slope of the straight line in the neighbourhood of E_{ocp}). This was done every 10 minutes from $t=0$ and $t=30\text{min}$: $t=0$ (immersion of the electrode) $+2\text{ min}$ (half of experiment since its duration is 4 min), $t=10 + 2\text{ min}$ (half of experiment) and $t=20 + 2\text{ min}$ (half of experiment)

Tafel experiment: measurement of the new E_{ocp} than potential increase from $E_{ocp} - 250\text{mV}$ up to E_{ocp} at $+1\text{mV/s}$ from E_{ocp} at $t=30\text{ min}$ (duration: from $t=30\text{ min}$ to $t=30\text{ min}+500\text{ seconds}$). This aimed to specify accurately the values of the corrosion potential (E_{corr}) and of the current density of corrosion (I_{corr}), and also to get the values of the anodic and cathodic Tafel coefficients (β_a and β_c).

These electrochemical experiments were performed in a very simple solution simulating saliva (distilled water added with 9g/L NaCl and pH adjusted to 7.4 just before experiment). Its temperature was maintained at 37°C thanks to a special cell allowing the heating by internal fluid circulation from a Julabo F32 device. The Working Electrode (the sample) was 1200-grit ground just before immer-

TABLE 1 : Chemical composition of the Co-15Cr alloy (full frame)

Co-15Cr alloy	AVERAGE	std deviation
wt.%Co	84.11	0.17
wt.%Cr	15.89	0.17

TABLE 2 : Chemical composition of the Co-30Cr alloy (full frame)

Co-30Cr alloy	AVERAGE	std deviation
wt.%Co	69.29	0.17
wt.%Cr	30.71	0.17

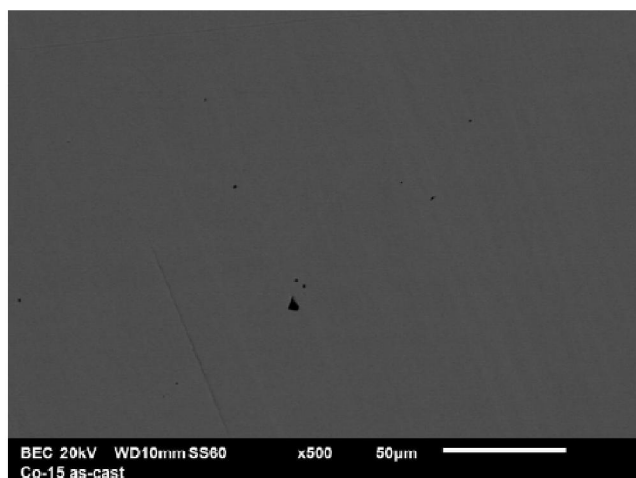
sion and each electrochemical series of experiments (3 liner polarization and Tafel), the Counter Electrode (or auxiliary electrode) was a platinum one, and the electrode of potential reference was a Saturated Calomel one.

RESULTS AND DISCUSSION

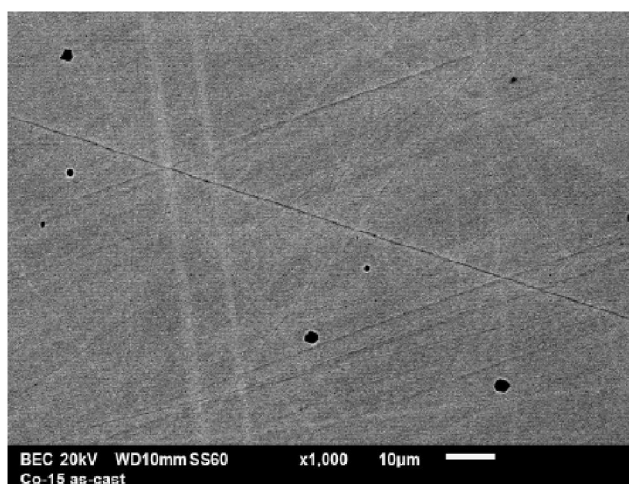
Chemical compositions and microstructures of the obtained alloys; hardness

The chemical compositions of the two alloys, as analysed using the SEM and its EDS device, are globally well respected (TABLE 1 and TABLE 2), despite a chromium content a little higher than expected. The as-cast microstructures of both alloys seem logically single-phased, as suggested in the SEM/BSE micrographs in Figure 1. No detectable chemical segregation can be noted.

The volumes and masses of the samples devoted



Co-15Cr alloy (as-cast)



Co-30Cr alloy (as-cast)

Figure 1 : The microstructures of the two studied alloys as observed with the SEM in BSE mode

Full Paper

TABLE 3 : Estimated values of the volume masses of the two alloys

Co-15Cr alloy	Co-30Cr alloy
density (g cm ⁻³)	density (g cm ⁻³)
8.31	8.33

TABLE 4 : Vickers hardness of the two alloys

Hardness (Hv10kg)	Co-15Cr	Co-30Cr
AVERAGE	417.0	204.7
Standard deviation	11.3	18.1

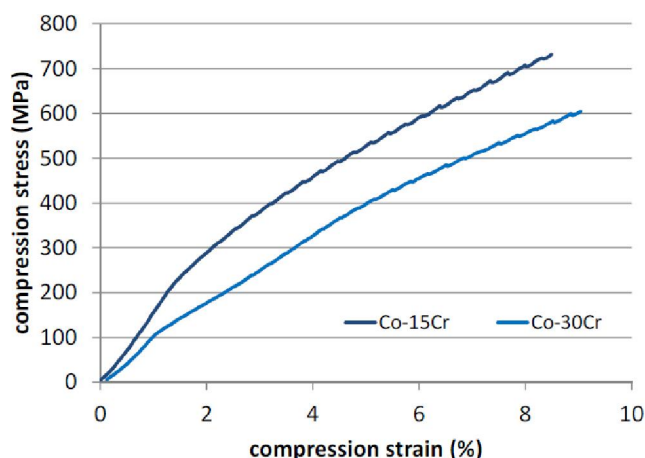


Figure 2 : The compression curves of the two studied alloys

to the compression tests were exploited to estimate their densities. The values given in TABLE 3 show that there is no real influence of the chromium content on the density. These densities, around 8.3, which are effectively very close to one another, are a little higher than the ones (8.1) of the two nickel-based dental alloys recently studied^[12].

The indentation runs performed on the two alloys led to the values presented in TABLE 4. The Co-15Cr alloy is obviously much harder than the 30wt.%Cr-containing one since the average value from three indentation is twice.

Mechanical properties in compression

The two alloys were subjected to compression test until reaching 8.5 to 9% of total deformation. The corresponding curves are plotted together in Figure 2. As for the nickel alloys recently studied with the same apparatus^[12], they are rather irregular with the same two parts of elastic deformation, especially in the case of the Co-30Cr alloy. The val-

TABLE 5 : The values of the elastic resistance of the alloys and of the maximal stresses at which the the compression were interrupted

Co-15Cr alloy	Co-30Cr alloy
Yield strength (MPa)	
343	320
Maximal stress applied (MPa)	
732	605

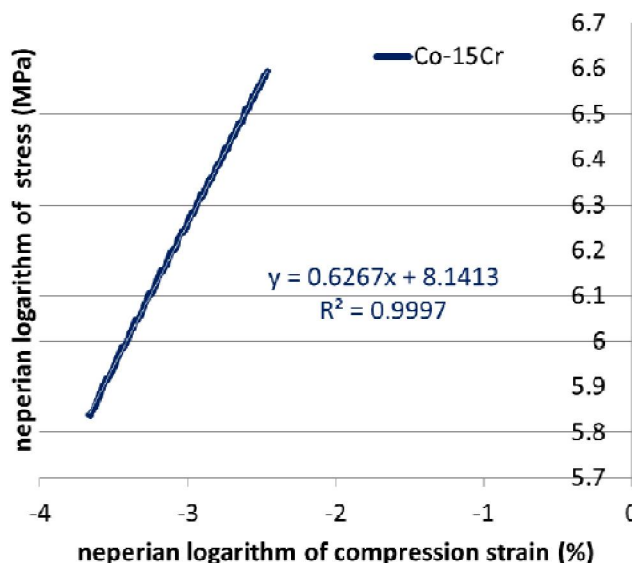


Figure 3 : Determination of the values of the hardening parameters of the Co-15Cr alloy

ues of the yield strengths and of the stresses at which the compression tests were interrupted are given in TABLE 5. The Co-15Cr alloy seems more resistant against compression than the Cr30Cr one (e.g. 20MPa more for the yield strength).

In contrast, the hardening parameters describing consolidation in the Ludwig's law (eq. 1) and issued from the graphs plotted according to (eq. 2) in Figure 3 and Figure 4, do not obviously depend on the chromium content (TABLE 6).

The plastic deformation led to the permanent relative deformations whose values are given in TABLE 7. Along the compression axis the permanent deformation is logically negative, but the absolute values are not the same (-3.9% for Co-15Cr and -6.1% for Co-30Cr). Thus the properties for the two alloys cannot be compared to one another for the deformed states.

Behaviour in corrosion

The results of linear polarization are displayed

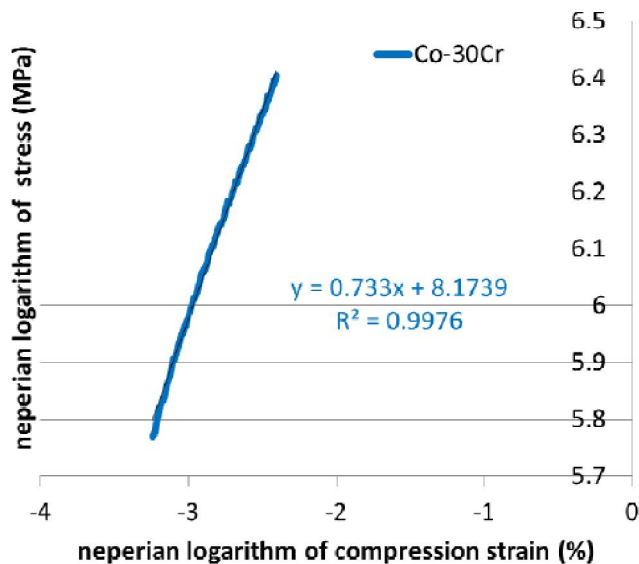


Figure 4 : Determination of the values of the hardening parameters of the Co-30Cr alloy

TABLE 6 : The values of the parameters of the Ludwig's equation describing the hardening parts of the curves

Hardening constants ($\sigma = k \times \epsilon^n$)	Co-15Cr	Co-30Cr
k (MPa)	3433	3547
n	0.627	0.733

TABLE 7 : Longitudinal and lateral deformations of the two samples after the deformation tests

Alloy	Relative longitudinal deformation (ϵ_{xx})	Relative lateral deformations (ϵ_{yy} and ϵ_{zz})
Co-15Cr	-3.88%	+1.24% and -0.80%
Co-30Cr	-6.06%	+2.56% and +3.32%

in TABLE 8 for the Co-15Cr alloy and in TABLE 9 for the Co-30Cr alloy. One can see first that both alloys are very corrosion-resistant with their very high values of R_p (several hundreds of $k\Omega \times cm^2$, and even $1 M\Omega \times cm^2$). However one must note that the not deformed Co-30Cr, despite both its highest Cr content and the fact it was not deteriorated by plastic deformation, shows the worst behaviour among the four electrodes. But it is true that, despite polarization resistances lower than $100 k\Omega \times cm^2$, the level of R_p remains very high.

The Tafel experiments led to curves which are displayed in Figure 5 (Co-15Cr not deformed and in the deformed state), Figure 6 (Co-30Cr not de-

TABLE 8 : The recorded open circuit potential and measured polarization resistance of the Co-15Cr alloy versus time

Co-15Cr (ND)	t = 0 min	t = 10 min	t = 20 min
E_{ocp}/HNE (mV)	*	-407.3	-388.7
R_p ($k\Omega \times cm^2$)	*	758.7	987.3

Co-15Cr (DF)	t = 0 min	t = 10 min	t = 20 min
E_{ocp}/HNE (mV)	*	-217.2	-201.4
R_p ($k\Omega \times cm^2$)	*	654.9	1007

TABLE 9 : The recorded open circuit potential and measured polarization resistance of the Co-30Cr alloy versus time

Co-30Cr (ND)	t = 0 min	t = 10 min	t = 20 min
E_{ocp}/HNE (mV)	*	-527.4	-524.6
R_p ($k\Omega \times cm^2$)	*	66.75	115.5

Co-30Cr (DF)	t = 0 min	t = 10 min	t = 20 min
E_{ocp}/HNE (mV)	*	-375.1	-368.7
R_p ($k\Omega \times cm^2$)	*	456.6	792.7

formed and in the deformed state) and Figure 7 (Co-15Cr and Co-30Cr in their not deformed state). The Tafel curves for the two alloys in their deformed states are also presented together, in Figure 8, despite that the deformation rates are not the same.

Observing the relative positions, vertically (corrosion potential) or horizontally (current density of corrosion) does not reveal any systematic hierarchy among the obtained results. In contrast, Tafel calculations, the results of which are displayed in TABLE 10 for the Co-15Cr alloy and in TABLE 11 for the Co-30Cr alloy, suggest that the Co-15Cr curiously behaves better than the Co-30Cr alloy whatever the deformed state (not deformed or plastically deformed) and that the hardening (deformed state) ought improving the corrosion resistance of each alloy. This fact, already suggested above by the values of polarization resistance, is rather surprising since in both case these were the inverse hierarchy which was expected.

General commentaries

By considering the all the results presented above the Co-15Cr alloy appears as being better than the Cr-richest one in all fields, mechanical and chemical. Indeed its hardness is higher and its compression behavior superior, and its resistance to corro-

Full Paper

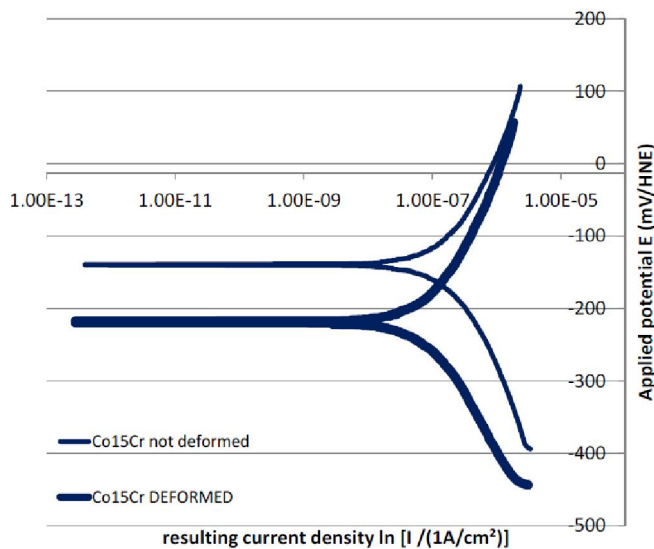


Figure 5 : The Tafel curves obtained for the Co-15Cr alloy for its not deformed state and in its deformed state

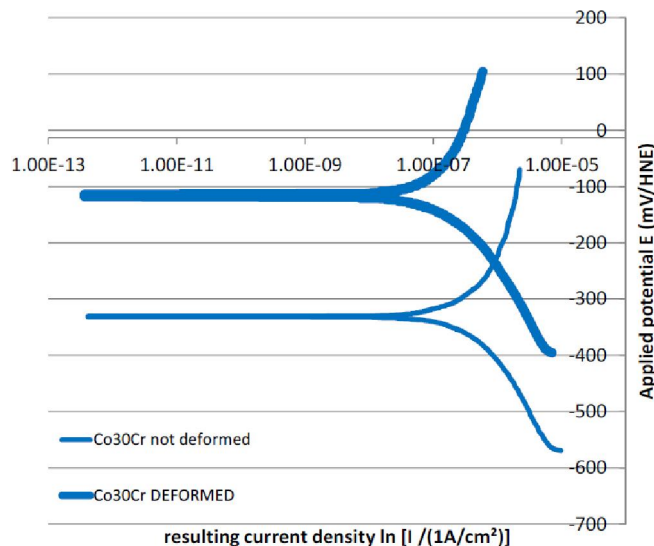


Figure 6 : The Tafel curves obtained for the Co-30Cr alloy for its not deformed state and in its deformed state

TABLE 10 : The values of E_{corr} , I_{corr} and of the Tafel anodic and cathodic coefficients for the Co-15Cr alloy in its initial state and in its deformed state

Co-15Cr Not Deformed			
E_{corr} /ENH (mV)	I_{corr} (nA/cm ²)	β_a (mV/decade)	β_c (mV/decade)
-379.5	235.4	230.9	218.9
Co-15Cr Plastically Deformed			
E_{corr} /ENH (mV)	I_{corr} (nA/cm ²)	β_a (mV/decade)	β_c (mV/decade)
-219.6	100.0	197.0	178.4

sion also better. The first finding is easily explainable by the intrinsic high hardness of pure cobalt by

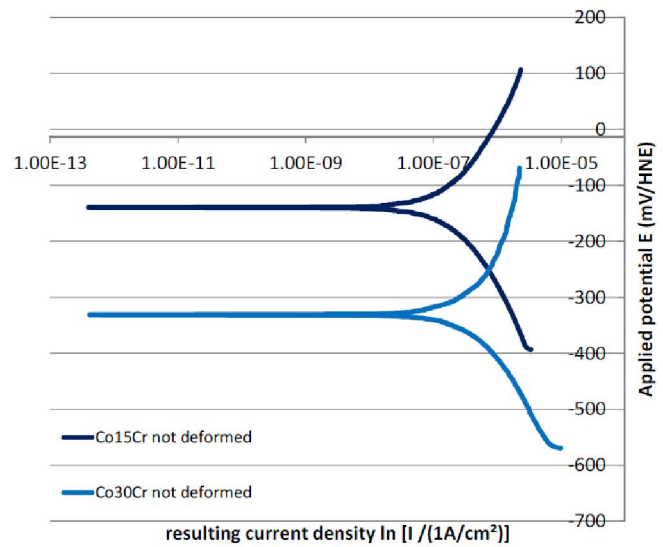


Figure 7 : The Tafel curves obtained for the Co-15Cr and Co-30Cr alloys for in their not deformed states

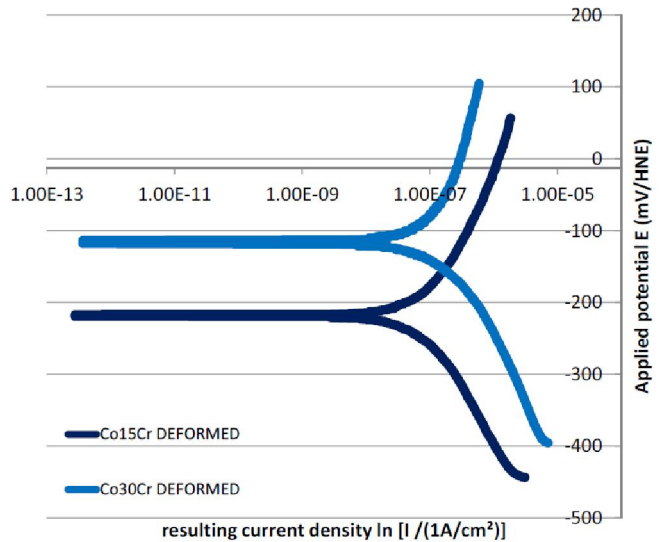


Figure 8 : The Tafel curves obtained for the Co-15Cr and Co-30Cr alloys for in their deformed states

TABLE 11 : The values of E_{corr} , I_{corr} and of the Tafel anodic and cathodic coefficients for the Co-30Cr alloy in its initial state and in its deformed state

Co-30Cr Not Deformed			
E_{corr} /ENH (mV)	I_{corr} (nA/cm ²)	β_a (mV/decade)	β_c (mV/decade)
-552.6	1250	336.6	248.5
Co-30Cr Plastically Deformed			
E_{corr} /ENH (mV)	I_{corr} (nA/cm ²)	β_a (mV/decade)	β_c (mV/decade)
-113.9	216.3	593.9	179.5

comparison to chromium, but the second was not expected because inverse to what is commonly

thought. Consequently one can imagine that enriching a {Co-15Cr}-based alloy with additional elements to improve its general properties, including the specific qualities required by a prosthetic use, may be more interesting than starting from a Co-30wt.%Cr base. The best corrosion resistance was observed for the plastically compressed sample for the two compositions. This is also rather surprising since one generally tends thinking that a deteriorated alloy is probably more threatened by corrosion.

CONCLUSIONS

Despite that this mechanical and corrosion study was carried out on two very simple alloys, it led to interesting, and sometimes surprising, observations. The differences in mechanical properties are easily explainable but, in contrast, the increases in corrosion resistance resulting from a lowering of the chromium content and of a preliminary plastic deformation remain to be verified, by reproducing the tests in more complex artificial saliva and by varying its content in dissolved oxygen. Intermediate values of chromium content on the one hand, and of hardening rate on the other hand, should confirming or not, and in the first case completing, the study.

ACKNOWLEDGMENTS

The authors thank Mathieu Lierre for the preparation of the solution as well as for its assistance.

REFERENCES

- [1] A.Marti; Injury, 31 Suppl., 418 (2000).
- [2] T.Yabuki, J.Ooe; Patent JP 61003860 A 19860109 (1986).
- [3] X.H.Zhang, C.F.Cui, X.Q.Zhang, Y.Jin; Kouqiang Yixue, **32(10)**, 613 (2012).
- [4] Y.Ren, K.Xiao, C.Shao, K.Yang, D.Zhan; Patent CN 103233143 A 20130807 (2013).
- [5] C.Laichici, V.Tirziu; Stomatologia (Buscharest), **15(5)**, 395 (1968).
- [6] B.Ghiban, C.Bortun, S.Ciucu; Analele Universitatii "Dunarea de Jos" din Galati, Fascicula IX : Metalurgie si Stiinta Materialelor, **26(2)**, 27 (2008).
- [7] O.Lingstuyt, B.Lavelle, F.Dabosi; Metall.Dent., Trav.Congr.Int., 348 (1981).
- [8] H.Hero, M.Syverud, J.Gloennes, J.A.Horst; Biomaterials, **5(4)**, 201 (1984).
- [9] M.Pourbaix; Biomaterials, **5(3)**, 122 (1984).
- [10] A.S.Corroy, P.Berthod, L.Aranda, P.De March; Materials Science: An Indian Journal, **12(7)**, 250 (2015).
- [11] A.S.Corroy, P.Berthod, P.De March; Materials Science: An Indian Journal, **12(11)**, 387 (2015).
- [12] L.P.Billy Nsougui, P.Berthod; Materials Science: An Indian Journal, *submitted*.